European Review for Medical and Pharmacological Sciences 2022; 26: 225-231

Corpus callosum volumetrics and clinical progression in early multiple sclerosis

M.A. SOTGIU[1], G. PIGA[2], V. MAZZARELLO[1], I.R. ZARBO[3], A. CARTA[4], L. SADERI[5], S. SOTGIU[4], M. CONTI[6], L. SABA[7], P. CRIVELLI[2]

[1]Department of Biomedical Sciences, University of Sassari, Sassari, Italy
[2]Azienda Ospedaliero Universitaria di Sassari, Institute of Diagnostic Imaging 2, Sassari, Italy
[3]Department of Clinical, Surgery and Experimental Sciences, Section of Neurology, University of Sassari, Sassari, Italy
[4]Department of Clinical and Experimental Medicine, Unit of Child Neuropsychiatry, University of Sassari, Sassari, Italy
[5]Department of Medical, Surgical and Experimental Sciences, Clinical Epidemiology and Medical Statistics Unit, University of Sassari, Sassari, Italy
[6]Department of Clinical and Experimental Medicine, Institute of Diagnostic Imaging 2, University of Sassari, Sassari, Italy
[7]Department of Radiology, Azienda Ospedaliero Universitaria di Cagliari, Cagliari, Italy

Abstract. – OBJECTIVE: Corpus callosum (CC) is commonly affected in multiple sclerosis (MS), with known association between CC atrophy and MS clinical activity. In this study, we assessed the association of callosal atrophy, lesions volume and residual CC volume with the clinical disability of early MS patients.

SUBJECTS AND METHODS: Thirteen MS subjects (9 female, mean age 36.9 years), studied with magnetic resonance imaging (MRI) were selected. MRI scans were performed at baseline (T_0), at 6 (T_1), 12 (T_2), and 24 months (T_3) from baseline. CC was segmented into three sections (genu, body, and splenium); callosal boundaries were outlined and all CC lesions were manually traced. Normal CC and CC lesion volumes were measured using a semiautomatic software.

RESULTS: From January 2014 to December 2016, all selected patients had confluent lesions on MRI at T3 with a significant increase in the size of confluent lesions compared to baseline (*p*=0.0007). At T1, a significant increase in the size of confluent (*p*=0.02) and single lesions located in the callosal body (*p*=0.04) was detected in patients with EDSS ≥1.5. Also, CC residual volume (CCR) rather than the whole CC volume (CCV) significantly correlated (*p*=0.03) with the clinical progression of MS in the whole cohort.

CONCLUSIONS: In early MS patients with higher EDSS at baseline, a significant increase in confluent CC lesions size is evident, particularly in the callosal body. Also, median CCR is significantly associated with MS progression in the whole MS group, regardless of initial EDSS. Given their significant association with disability, we encourage measuring CC body lesions and residual CC size for therapeutic decisions and prognostic planning in early MS.

Key Words:

Corpus callosum, Volume, Multiple sclerosis, Demyelinating lesions, MRI.

Introduction

Multiple sclerosis (MS) is an immune-mediated disorder of the central nervous system, characterized by inflammation, demyelination and axonal loss. It is a frequent cause of neurological disability in young adults[1].

The corpus callosum (CC) is of peculiar interest in MS: with up to 250 million transversely oriented nerve fibers, CC is the largest commissural white matter tract connecting cortical and subcortical regions with the two brain hemispheres[2]. CC lesions occur in up to 95% of MS patients and may strongly contribute to the development of both physical and cognitive impairments[3]. Moreover, being composed of long inter-hemispheric fibers, CC may be representative of the changes in white matter occurring in the MS brain[4].

MS diagnosis is mainly based on magnetic resonance imaging (MRI)[5-8], which is central also for prognostic purposes[9,10]. Large cohort studies disability[11-14] have shown association between CC lesions and CC atrophy and between CC atrophy and increased disease activity, which could help identify patients at high risk of future. Strategies have been developed to measure CC atrophy, from bidimensional approaches to more advanced volumetric techniques[15-17].

Corresponding Author: Stefano Sotgiu, MD; e-mail: stefanos@uniss.it

The purpose of the current study was to assess the relationship between CC atrophy, normal residual callosal volume (CCR) and CC lesions volume with the disability accumulation in selected MS patients at their early stage of disease.

Subjects and Methods

Subjects

In this retrospective study, 13 subjects who underwent MRI for diagnostic purposes from January 2014 to December 2016 were included. Inclusion criteria: age 18 years, MS diagnosis according to revised McDonald criteria[6-8], and MRI scans performed at baseline (T_0), at 6 (T_1), 12 (T_2) and 24 months from baseline (T_3). Patients were excluded if additional diagnoses were present and if MRI analyses did not comply with the strict chronology. Age, gender, symptoms at onset, age at MS diagnosis, disease course[18], Expanded Disability Status Scale (EDSS) and disease modifying treatments were also obtained from clinical files.

MRI Analysis and Segmentation

All MRIs were performed with a standardized protocol using a 1.5 T scanner Philips Achieva® (Best, Netherlands). Sagittal FLAIR sequences (repetition time [TR] = 4800 ms; echo time [TE] = 297 ms; -0.6 continuous, 1.5-mm-thick, axial slices; matrix size = 200 × 200; field of view [FOV] = 240 × 240 mm^2) were examined at the different time points. Each acquisition was performed with special care to identify the correct alignment to have an optimal spatial co-registration.

The DICOM datasets were analyzed with the software 3D Slicer 4.10.1 (the open-source software platform is available at https://www.slicer.org). Two experienced neuroradiologists (PG and CP with 5 and 11 years in neuroimaging, respectively), blinded on clinical information, performed MRI analysis and segmentation according with standardized methods[19-22] (Figure 1).

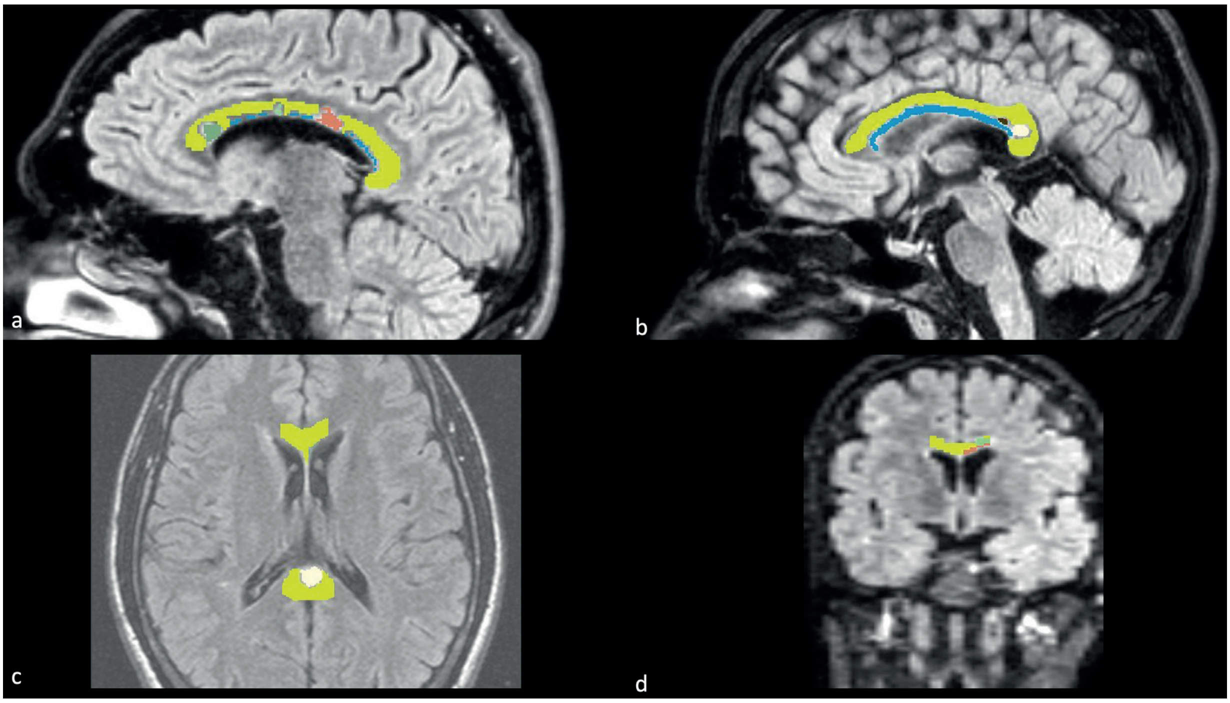

Figure 1. Representative CC contouring and segmentation on four different MS subjects. A 30 y/o male subject (panel a) FLAIR-sequence, sagittal view; corpus callosum contoured with different color: dark green (*lesion localized anteriorly, at genu level*), light green (*lesion localized in the middle of the body*), light brown (*lesion located more posteriorly in the body*) and light blue (*confluent lesion*); yellow represents the *corpus callosum residual*. For each slice the lesions were outlined first, and then, the corpus callosum residual. A 21 y/o female subject (panel b) FLAIR-sequence, sagittal view: in light blue extended *confluent lesion*[30]; in the splenium, *two further lesions* are detectable (dark brown and white), in yellow the *corpus callosum residual*. A 36 y/o male subject, same of panel (panel c). FLAIR-sequence, axial view: a *demyelinating lesion at the level of splenium is clearly visible* in white. In yellow the *corpus callosum residual*. Axial images, as well as the coronal ones, were used to check the contour performed in sagittal. A 19 y/o female subject same of panel b (panel d). FLAIR-sequence, coronal view: two distinct lesions are visible, *one more caudal and medial* in light brown and *one more cranial, at the left lateral limit of the corpus callosum*, in light green; in yellow the *corpus callosum residual*

Table I. Demographic and descriptive analysis.

Variables	
Female, n (%)	9/13 (69.2)
Mean (SD) age, years (n= 13)	41.5 (14.4)
Mean (SD) age at MS onset, years (n= 13)	36.9 (14.4)
Course, n (%)	
RR	12/13 (92.3)
RP	1/13 (7.7)
DMT, n (%)	
None	4/13 (30.8)
IFNβ-1a	3/13 (23.1)
Glatiramer acetate	2/13 (15.4)
Natalizumab	2/13 (15.4)
Dimethyl fumarate	1/13 (7.7)
IFNβ-1b	1/13 (7.7)

DMT: Disease modifying treatments; **RR:** relapsing-remitting; **RP:** relapsing-progressive; **IFN:** interferon.

Following Cai et al[22], CC was segmented into three sections, corresponding to genu, body and splenium: the rostrum was merged with the genu and the isthmus with the body. Callosal boundaries were outlined using the "Editor" module of 3D Slicer. All CC lesions were manually traced and painted. A numeric code was assigned to each of them to identify the different type of lesion (single or confluent) and their location within the three parts of CC. The measurements of the following parameters were obtained: CCV (total volume of CC), SL (single lesion), CL (confluent lesion) and CCR (corpus callosum residual, i.e., CCV minus single and confluent lesions).

Manual segmentation of the outer boundaries was performed slice by slice on sagittal planes, with a further check on axial and coronal view to correct potential contouring mistakes. Most cranial and most caudal slices were excluded to avoid volume artefacts. Finally, a table containing data on CC volumes was generated and measures expressed as cubic centimeters (cc).

Statistical Analysis

An *ad hoc* electronic form was used to collect all the variables in the study. Qualitative variables were described with absolute and relative (percentage) frequencies; quantitative variables were summarized with means (standard deviations, SD) or medians (interquartile ranges, IQR) in the case of parametric and non-parametric distribution, respectively. Qualitative variables were compared with Chi-squared or Fisher's exact test when appropriate. Mann-Whitney or Student's *t*-test were used to detect statistical differences in the comparison of non-parametric or parametric variables, respectively. The one-way analysis of variance (ANOVA) and Friedman's test were performed to detect differences of quantitative variables at different time points depending on parametric and non-parametric distribution, respectively. A two-tailed p-value < 0.05 was considered statistically significant. The statistical software STATA version 16 (StataCorp, TX, USA) was used to perform all statistical computations.

Results

Demographic and clinical characteristics of the patients (69.2% females) are summarized in Table I. Mean age at disease onset was 36.9 years. Twelve out of thirteen patients (92.3%) had a relapsing-remitting (RR) course. Median EDSS score significantly worsened in all patients from baseline (1.5) to month 24 (3.0; p=0.005; Table II).

Table II. Comparison of variables from baseline to T_3.

Variables	T_0	T_1	T_2	T_3	p
EDSS§	1.5 (1.0-2.5)	1.5 (1.5-4)	3 (1.5-3.5)	3 (1.5-4)	0.005*
CCR (cc)§	10.5 (9.2-12.6)	10.08 (9.3-10.9)	9.4 (8.3-10)	9.52 (7.8-10.1)	0.03**
SPLENIUM SL (cc)§	0.12 (0.08-0.2)	0.1 (0.07-0.12)	-	0.03 (0.02-0.04)	n.a.
BODY SL (cc)§	0.09 (0.02-0.5)	0.12 (0.04-0.2)	0.09 (0.02-0.2)	0.1 (0.04-0.1)	0.75
GENU SL (cc)§	0.14 (0.12-0.4)	0.1 (0.1-0.2)	-	-	0.18
CL (cc)§	0.8 (0.27-1.02)	1.02 (0.7-1.28)	1.07 (0.7-1.2)	1.15 (0.8-1.2)	0.007***
Mean (SD) CCV (cc)	12.1 (±2.6)	11.8 (±2.3)	10.5 (±1.4)	10.5 (±1.8)	0.10

EDSS: Expanded Disability Status Scale; **CCR:** corpus callosum residual; **SL:** single lesions; **CL:** confluent lesions; **CCV:** corpus callosum volume; **cc:** cubic centimetres; **n.a.:** not applicable; **§:** Median value (interquartile range)

**T_0 vs. T_2= 0.01; T_0 vs. T_3= 0.02.*

***T_0 vs. T_2= 0.009; T_0 vs. T_3= 0.03; T1 vs. T2= 0.006.*

****T_0 vs. T_1= 0.03; T_0 vs. T_2= 0.006; T0 vs. T3= 0.0006.*

At T_0, 46.1% of subjects had T2/FLAIR-weighted hyperintense lesions in the splenium, 23.1% in the body and 23.1% in the genu of the CC.

At T_3, all patients had CL on CC which were significantly larger compared to the previous time points (p=0.007). On the contrary, no significant mean CCV decrease was detected over time (Table II).

Regarding CCR, the median volume was 10.5 cc at baseline and 9.5 cc at T_3 (p=0.03). CCR volume was also significantly reduced at T_2 (p=0.009) and when comparing T_1 with T_2 (p=0.006) (Table II and Figure 2). Immunomodulatory treatments (listed on Table I) did not significantly influence disability accumulation, nor the whole CC volume or the volume of CC lesions (not shown).

Finally, stratifying according to the median EDSS at onset, already at T_1 there was a statistically significant size increase of the callosal body lesions (p=0.04) and of the CL (p=0.02) in those patients with baseline EDSS ≥1.5 (Table III). This tendency was maintained throughout the whole observational period.

Discussion

In the last 20 years, CC has attracted great interest in neuroimaging for its prognostic role in neurodegenerative disorders[23,24]. Having demarcated two-dimensional limits on mid-sagittal T1-weighted imaging, CC can be easily identified on conventional MRI[25] for manual measures of its atrophy[26]. We adopted a semiautomatic software to evaluate the relationship between callosal volume reduction on MRI and clinical changes in a cohort of MS patients. We took special care to ensure the reproducibility of CC volume and sub-components on MRI, as suggested[19].

A timely detection of callosal atrophy in patients at their first demyelinating attack can predict the development of definite MS[26,27]. Our results suggested that CC residual volume (CCR), rather than CC global atrophy, is progressively reduced (T_1-T_3) during the initial MS stages[3,22-25]. On the contrary, no association was found between the atrophy of the whole CC and disability accumulation, neither in the entire MS group nor when stratifying patients according to EDSS severity at onset. In our study, CCR (i.e., the CCV minus the single and confluent lesions) does not reflect the increase in CC lesions volume. This can be attributed to the removal of confounding factors, such as the inflammatory lesional edema and the spurious augmentation of CC volume. Studies over the last 10 years confirmed the uncertain relationship between CC atrophy and disability: a moderate correlation is reported in some studies, but not in others[28,29]. Also, the volume of CC lesions, particularly those in the CC body, increased at T_1 and significantly progressed over the following years in patients with higher EDSS at onset. Therefore, in addition to CCR, we may also propose a prognostic role to the callosal body lesions[23-29].

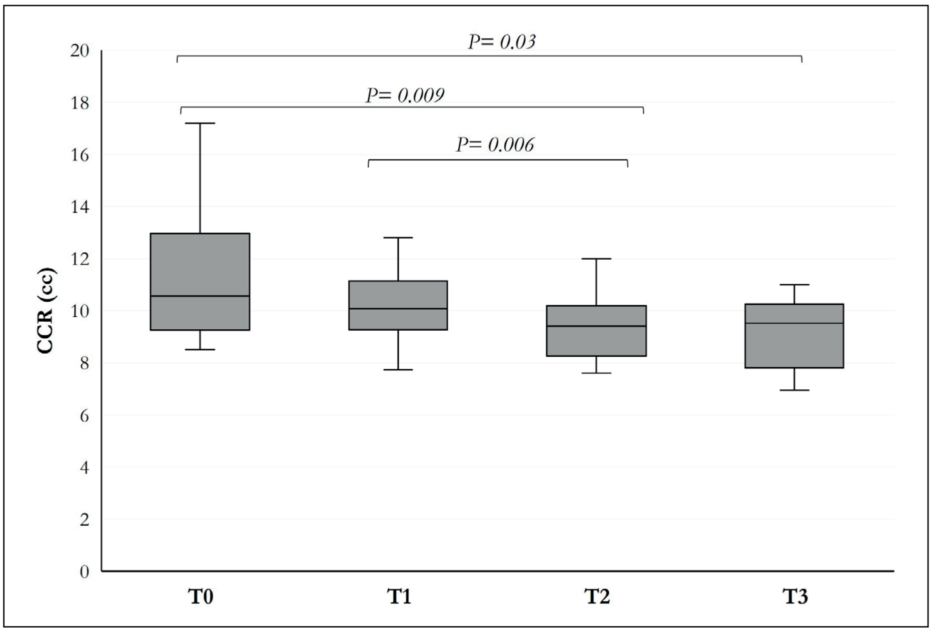

Figure 2. CCR median values from baseline to T_3 in the whole MS cohort. Comparison of CCR volumes between T_0 (baseline) and T_2 (12 months) showed a significant decrease (p=0.009) as well as that between T_1 (6 months) and T_2 (p=0.006) and between T_0 and T_3 (24 months; p=0.03). Detailed median CCR values and interquartile ranges are reported in the text.

Table III. Stratification of variables according to EDSS at baseline.

Variables	EDSS <1.5 (n= 6)	EDSS ≥1.5 (n= 7)	*p*-value
Female, n (%)	5 (83.3)	4 (57.1)	n.s.
Mean (SD) age, y	39.3 (10.6)	43.4 (17.8)	n.s.
Mean (SD) age at onset, y	34.5 (10.8)	38.9 (17.6)	n.s.
Course, n (%)			
RR	6 (83.3)	6 (85.7)	n.s.
PR	-	1 (14.3)	
EDSS at T1§	1.3 (1.0-2.5)	4.0 (1.5-5.5)	0.05
EDSS at T2§	2.0 (1.0-3.0)	3.5 (2.0-5.5)	0.08
EDSS at T3§	1.3 (1.0-3.5)	3.5 (2.0-5.5)	0.08
T_0			
CCR (cc)§	11.5 (9.9-15.0)	9.3 (8.8-12.6)	n.s.
SPLENIUM SL (cc)§	0.20 (0.16-0.57)	0.08 (0.03-0.08)	0.05
BODY SL (cc)§	0.06 (0.02-0.09)	0.51 (-)	n.s.
GENU SL (cc)§	0.14 (-)	0.26 (0.12-0.39)	n.s.
CL (cc)§	0.58 (0.32-1.10)	0.9 (0.16-1.02)	n.s.
Mean (SD) CCV (cc)	13.1 (2.9)	11.3 (2)	n.s.
T_1			
CCR (cc)§	10.7 (9.2-12.8)	9.7 (9.4-11)	n.s.
SPLENIUM SL (cc)§	0.10 (0.05-0.30)	0.1 (0.08-0.1)	n.s.
BODY SL (cc)§	0.04 (0.01-0.06)	0.2 (0.16-0.3)	**0.04**
GENU SL (cc)§	0.10 (-)	0.22 (-)	n.s.
CL (cc) §	0.73 (0.55-0.82)	1.2 (1.06-1.6)	**0.02**
Mean (SD) CCV (cc)	12.3 (3.1)	11.3 (1.4)	n.s.
T_2			
CCR (cc)§	9.1 (8.54-10.34)	9.4 (8.2-10.04)	n.s.
SPLENIUM SL (cc)§	0.03 (-)	0.15 (-)	n.s.
BODY SL (cc)§	0.02 (-)	0.1 (0.09-0.19)	0.05
GENU SL (cc)§	-	0.14 (-)	-
CL (cc)§	0.96 (0.75-1.36)	1.07 (0.9-1.2)	n.s.
Mean (SD) CCV (cc)	10.6 (1.7)	10.5 (1.2)	n.s.
T_3			
CCR (cc)§	9.2 (7.80-10.37)	9.5 (7.8-10.1)	n.s.
SPLENIUM SL (cc)§	0.03 (0.02-0.04)	0.04 (-)	n.s.
BODY SL (cc)§	0.01 (0.01-0.08)	0.15 (0.1-0.17)	0.05
GENU SL (cc)§	-	0.19 (-)	-
CL (cc)§	0.88 (0.70-2.31)	1.1 (1.01-1.25)	n.s.
Mean (SD) CCV (cc)	10.5 (2.2)	10.5 (1.5)	n.s.

EDSS: Expanded Disability Status Scale; **CCR:** corpus callosum residual; **SL:** single lesions; **CV:** confluent lesions; **CCV:** corpus callosum volume; **cc:** cubic centimetres; **n.s.:** not significant; **y:** years; **§:** Median value (interquartile range).

Finally, we acknowledge some limitations in this study. First, it has a retrospective cross-sectional nature, and it includes a limited cohort of patients (due to the strict temporal and alignment criteria). A larger, prospective study would be important to confirm these preliminary results. Second, MRI analysis was limited to CC, with no other brain and spinal regions investigated. We also quantified CC volume semi-automatically drawing CC contour on non-isotropic images, while a fully automated approach on isotropic images would be the gold standard for volumetric determinations. However, we consider this a minor limitation due to the high value of reproducibility reported in the literature and the strict adherence to the alignment plane that has been followed.

Conclusions

The reduction of CCR and the increase of confluent lesions in the CC body are associated with higher disability risk in MS. Our findings strengthen the idea that focal variations of callosal lesions in early MS stages may be central for developing proper treatment planning. Larger studies are needed to confirm CC as a reliable prognostic biomarker in MS.

Acknowledgments

Thanks to Elisa Sotgiu and Thomas Leonard-Roy, Departments of Comparative Literature and English, Harvard University, Cambridge, MA (USA) for help with proofreading.

Ethical Approval and Informed Consent

All procedures performed in the studies involving human participants were in accordance with the Ethical Standards of the Institutional and/or National Research Committee and with the 1964 Helsinki Declaration and its later amendments or comparable ethical standards. For this type of study, informed consent is not required.

Consent for Publication

Not applicable.

Conflict of Interests

The authors declare that they have no competing interests.

Funding

This study was funded by "Fondo di Ateneo per la ricerca 2019", University of Sassari.

Authors' Contributions

MAS: study concept and design, literature research, manuscript preparation; GP: literature research, data analysis; VM: study design, literature research; IRZ: clinical data collection; AC: data collection, manuscript review and editing; LS: statistical analysis; SS: manuscript review and editing; MC: manuscript review; LS: manuscript review and editing; PC: data analysis and manuscript review. All authors read and approved the final manuscript.

References

1) Filippi M, Bar-Or A, Piehl F, Preziosa P, Solari A, Vukusic S, Rocca MA. Multiple sclerosis. Nat Rev Dis Primers 2018; 4: 43.
2) Mooshagian E. Anatomy of the corpus callosum reveals its function. J Neurosci 2008; 28: 1535-1536.
3) Bodini B, Cercignani M, Khaleeli Z, Miller DH, Ron M, Penny S, Thompson AJ, Ciccarelli O. Corpus callosum damage predicts disability progression and cognitive dysfunction in primary-progressive MS after five years. Hum Brain Mapp 2013; 34: 1163-1172.
4) Evangelou N, Konz D, Esiri MM, Smith S, Palace J, Matthews PM. Regional axonal loss in the corpus callosum correlates with cerebral white matter lesion volume and distribution in multiple sclerosis. Brain 2000; 123: 1845-1849.
5) Garg N, Reddel SW, Miller DH, Chataway J, Riminton DS, Barnett Y, Masters L, Barnett MH, Hardy TA. The corpus callosum in the diagnosis of multiple sclerosis and other CNS demyelinating and inflammatory diseases. J Neurol Neurosurg Psychiatry 2015; 86: 1374-1382.
6) Polman CH, Reingold SC, Banwell B, Clanet M, Cohen JA, Filippi M, Fujihara K, Havrdova E, Hutchinson M, Kappos L, Lublin FD, Montalban X, O'Connor P, Sandberg-Wollheim M, Thompson AJ, Waubant E, Weinshenker B, Wolinsky JS. Diagnostic criteria for multiple sclerosis: 2010 revisions to the McDonald criteria. Ann Neurol 2011; 69: 292-302.
7) Filippi M, Rocca MA, Ciccarelli O, De Stefano N, Evangelou N, Kappos L, Rovira A, Sastre-Garriga J, Tintorè M, Frederiksen JL, Gasperini C, Palace J, Reich DS, Banwell B, Montalban X, Barkhof F; MAGNIMS Study Group. MRI criteria for the diagnosis of multiple sclerosis: MAGNIMS consensus guidelines. Lancet Neurol 2016; 15: 292-303.
8) Thompson AJ, Banwell BL, Barkhof F, Carroll WM, Coetzee T, Comi G, Correale J, Fazekas F, Filippi M, Freedman MS, Fujihara K, Galetta SL, Hartung HP, Kappos L, Lublin FD, Marrie RA, Miller AE, Miller DH, Montalban X, Mowry EM, Sorensen PS, Tintoré M, Traboulsee AL, Trojano M, Uitdehaag BMJ, Vukusic S, Waubant E, Weinshenker BG, Reingold SC, Cohen JA. Diagnosis of multiple sclerosis: 2017 revisions of the McDonald criteria. Lancet Neurol 2018; 17: 162-173.
9) Audoin B, Ibarrola D, Malikova I, Soulier E, Confort-Gouny S, Duong MV, Reuter F, Viout P, Ali-Chérif A, Cozzone PJ, Pelletier J, Ranjeva JP. Onset and underpinnings of white matter atrophy at the very early stage of multiple sclerosis--a two-year longitudinal MRI/MRSI study of corpus callosum. Mult Scler 2007; 13: 41-51.
10) Uher T, Vaneckova M, Sobisek L, Tyblova M, Seidl Z, Krasensky J, Ramasamy D, Zivadinov R, Havrdova E, Kalincik T, Horakova D. Combining clinical and magnetic resonance imaging markers enhances prediction of 12-year disability in multiple sclerosis. Mult Scler 2017; 23: 51-61.
11) Figueira FF, Santos VS, Figueira GM, Silva AC. Corpus callosum index: a practical method for long-term follow-up in multiple sclerosis. Arq Neuropsiquiatr 2007; 65: 931-935.
12) Petracca M, Schiavi S, Battocchio M, El Mendili MM, Fleysher L, Daducci A, Inglese M. Streamline density and lesion volume reveal a postero-anterior gradient of corpus callosum damage in multiple sclerosis. Eur J Neurol 2020; 27: 1076-1082.

13) Filippi M, Rocca MA. The role of magnetic resonance imaging in the study of multiple sclerosis: diagnosis, prognosis and understanding disease pathophysiology. Acta Neurol Belg 2011; 111: 89-98.
14) Filippi M, Rocca MA, Barkhof F, Brück W, Chen JT, Comi G, DeLuca G, De Stefano N, Erickson BJ, Evangelou N, Fazekas F, Geurts JJ, Lucchinetti C, Miller DH, Pelletier D, Popescu BF, Lassmann H; Attendees of the Correlation between Pathological MRI findings in MS workshop. Association between pathological and MRI findings in multiple sclerosis. Lancet Neurol 2012; 11: 349-360.
15) Filippi M, Preziosa P, Banwell BL, Barkhof F, Ciccarelli O, De Stefano N, Geurts JJG, Paul F, Reich DS, Toosy AT, Traboulsee A, Wattjes MP, Yousry TA, Gass A, Lubetzki C, Weinshenker BG, Rocca MA. Assessment of lesions on magnetic resonance imaging in multiple sclerosis: practical guidelines. Brain 2019; 142: 1858-1875.
16) Kim KW, MacFall JR, Payne ME. Classification of white matter lesions on magnetic resonance imaging in elderly persons. Biol Psychiatry 2008; 64: 273-280.
17) Park G, Kwak K, Seo SW, Lee JM. Automatic Segmentation of Corpus Callosum in Midsagittal Based on Bayesian Inference Consisting of Sparse Representation Error and Multi-Atlas Voting. Front Neurosci 2018; 12: 629.
18) Lublin FD, Reingold SC, Cohen JA, Cutter GR, Sørensen PS, Thompson AJ, Wolinsky JS, Balcer LJ, Banwell B, Barkhof F, Bebo B Jr, Calabresi PA, Clanet M, Comi G, Fox RJ, Freedman MS, Goodman AD, Inglese M, Kappos L, Kieseier BC, Lincoln JA, Lubetzki C, Miller AE, Montalban X, O'Connor PW, Petkau J, Pozzilli C, Rudick RA, Sormani MP, Stüve O, Waubant E, Polman CH. Defining the clinical course of multiple sclerosis: the 2013 revisions. Neurology 2014; 83: 278-286.
19) Van Schependom J, Jain S, Cambron M, Vanbinst AM, De Mey J, Smeets D, Nagels G. Reliability of measuring regional callosal atrophy in neurodegenerative diseases. Neuroimage Clin 2016; 12: 825-831.
20) Herron TJ, Kang X, Woods DL. Automated measurement of the human corpus callosum using MRI. Front Neuroinform 2012; 6: 25.
21) Dworkin JD, Linn KA, Oguz I, Fleishman GM, Bakshi R, Nair G, Calabresi PA, Henry RG, Oh J, Papinutto N, Pelletier D, Rooney W, Stern W, Sicotte NL, Reich DS, Shinohara RT; North American Imaging in Multiple Sclerosis Cooperative. An Automated Statistical Technique for Counting Distinct Multiple Sclerosis Lesions. Am J Neuroradiol 2018; 39: 626-633.
22) Cai MT, Zhang YX, Zheng Y, Fang W, Ding MP. Callosal lesions on magnetic resonance imaging with multiple sclerosis, neuromyelitis optica spectrum disorder and acute disseminated encephalomyelitis. Mult Scler Relat Disord 2019; 32: 41-45.
23) Granberg T, Martola J, Bergendal G, Shams S, Damangir S, Aspelin P, Fredrikson S, Kristoffersen-Wiberg M. Corpus callosum atrophy is strongly associated with cognitive impairment in multiple sclerosis: Results of a 17-year longitudinal study. Mult Scler 2015; 21: 1151-1158.
24) Barkhof FJ, Elton M, Lindeboom J, Tas MW, Schmidt WF, Hommes OR, Polman CH, Kok A, Valk J. Functional correlates of callosal atrophy in relapsing-remitting multiple sclerosis patients. A preliminary MRI study. J Neurol 1998; 245: 153-158.
25) Miller DH, Barkhof F, Frank JA, Parker GJ, Thompson AJ. Measurement of atrophy in multiple sclerosis: pathological basis, methodological aspects and clinical relevance. Brain 2002; 125: 1676-1695
26) Pelletier J, Suchet L, Witjas T, Habib M, Guttmann CR, Salamon G, Lyon-Caen O, Chérif AA. A longitudinal study of callosal atrophy and interhemispheric dysfunction in relapsing-remitting multiple sclerosis. Arch Neurol 2001; 58: 105-111.
27) Kalincik T, Vaneckova M, Tyblova M, Krasensky J, Seidl Z, Havrdova E, Horakova D. Volumetric MRI markers and predictors of disease activity in early multiple sclerosis: a longitudinal cohort study. PLoS One 2012; 7: e50101.
28) Yaldizli O, Atefy R, Gass A, Sturm D, Glassl S, Tettenborn B, Putzki N. Corpus callosum index and long-term disability in multiple sclerosis patients. J Neurol 2010; 257: 1256-1264.
29) Yaldizli Ö, Penner IK, Frontzek K, Naegelin Y, Amann M, Papadopoulou A, Sprenger T, Kuhle J, Calabrese P, Radü EW, Kappos L, Gass A. The relationship between total and regional corpus callosum atrophy, cognitive impairment and fatigue in multiple sclerosis patients. Mult Scler 2014; 20: 356-364.
30) Cappelle S, Pareto D, Tintoré M, Vidal-Jordana A, Alyafeai R, Alberich M, Sastre-Garriga J, Auger C, Montalban X, Rovira À. A validation study of manual atrophy measures in patients with Multiple Sclerosis. Neuroradiology 2020; 62: 955-964.